

A Journal of the Gesellschaft Deutscher Chemiker

# Angewandte Chemie

GDCh

International Edition

[www.angewandte.org](http://www.angewandte.org)

## Accepted Article

**Title:** Blue Emissive Cobalt(III) Complexes and Their Use in the Photocatalytic Trifluoromethylation of Polycyclic Aromatic Hydrocarbons

**Authors:** Amlan K. Pal, Chenfei Li, Garry Shawn Hanan, and Eli Zysman-Colman

This manuscript has been accepted after peer review and appears as an Accepted Article online prior to editing, proofing, and formal publication of the final Version of Record (VoR). This work is currently citable by using the Digital Object Identifier (DOI) given below. The VoR will be published online in Early View as soon as possible and may be different to this Accepted Article as a result of editing. Readers should obtain the VoR from the journal website shown below when it is published to ensure accuracy of information. The authors are responsible for the content of this Accepted Article.

**To be cited as:** *Angew. Chem. Int. Ed.* 10.1002/anie.201802532  
*Angew. Chem.* 10.1002/ange.201802532

**Link to VoR:** <http://dx.doi.org/10.1002/anie.201802532>  
<http://dx.doi.org/10.1002/ange.201802532>

## COMMUNICATION

# Blue Emissive Cobalt(III) Complexes and Their Use in the Photocatalytic Trifluoromethylation of Polycyclic Aromatic Hydrocarbons

Amlan K. Pal,<sup>a,b</sup> Chenfei Li,<sup>b</sup> Garry S. Hanan<sup>\*a</sup> and Eli Zysman-Colman<sup>\*b</sup>

**Abstract:** The first examples of room temperature (r.t.) luminescent Co(III) complexes (**1** and **2**) are presented that exhibit intense ligand-to-metal and ligand-to-ligand charge transfer absorption in the low energy UV region ( $\lambda_{\text{abs}} \sim 360\text{-}400\text{ nm}$ ) and low-negative quasi-reversible reduction events ( $E_{(\text{red})}^{1/2} = -0.58\text{ V}$  and  $-0.39\text{ V}$  vs. SCE for **1** and **2**, respectively). The blue emission of **1** and **2** at r.t. is due to the large bite angles and strong  $\sigma$ -donation of the ligands, the combined effect of which helps to separate the emissive <sup>3</sup>LMCT (triplet ligand-to-metal charge transfer) and the non-emissive <sup>3</sup>MC (triplet metal-centered) states. **1** and **2** were found to be powerful photo-oxidants ( $E_{\text{Co(III)}/\text{Co(II)}} = 2.26\text{ V}$  and  $2.75\text{ V}$  vs. SCE of **1** and **2**, respectively) and were used as inexpensive photoredox catalysts for the regioselective mono(trifluoromethylation) of polycyclic aromatic hydrocarbons (PAHs) in good yields ( $\sim 40\text{-}58\%$ ).

The last decade has seen a renaissance in photochemistry as a tool to promote a wide range of organic transformations under mild conditions. Key to the popularity is the use of visible light with d<sup>6</sup> metal complexes, typically those based on Ru(II) and Ir(III), that act as photosensitizers/photoredox catalysts to initiate radical cascade reactions mediated by photo-induced electron transfer processes.<sup>1</sup> The excited state of these complexes is typically mixed charge-transfer (<sup>3</sup>CT) in nature with associated emission lifetimes on the sub-microsecond to microsecond regime. The toxicity, scarcity and associated elevated cost of these complexes has stimulated the search for replacement photocatalysts based on earth-abundant elements.<sup>2</sup> While there is a plethora of examples of photoactive 2<sup>nd</sup> and 3<sup>rd</sup> row transition metal complexes, there is a considerable dearth of photoactive 1<sup>st</sup> row complexes due to presence of low-lying metal-centered (<sup>3</sup>MC) states that deactivate the CT excited state.<sup>3</sup> Many strategies have been used to improve the photophysical properties of these complexes with the most popular focusing on the manipulation of the energies of non-emissive <sup>3</sup>MC states relative to emissive triplet metal-to-ligand charge transfer (<sup>3</sup>MLCT) states.<sup>4</sup> Some fruitful approaches to destabilize the energy of the <sup>3</sup>MC states

consist of (a) introduction of strong donor ligands and (b) the use of tridentate ligands that form 6-membered chelate rings to reduce the steric strain and achieve a more octahedral geometry compared to those bearing five-membered chelate rings. Following these approaches, Ru(II),<sup>5,6</sup> Cr(III)<sup>7</sup> and Fe(III, low spin)<sup>8</sup> complexes with strongly  $\sigma$ -donating tridentate ligands have been shown to have dramatically longer emission lifetimes. Another popular strategy to induce emission in 1<sup>st</sup> row transition metals is to use d<sup>10</sup> metal-ions to avoid non-emissive d-d transition, e.g., Cu(I)<sup>9</sup> Ni(0),<sup>10</sup> and Zn(II)<sup>11</sup>; however, their MLCT excited states often undergo strong geometrical distortion<sup>12</sup> and non-radiative relaxation to the ground state can be rapid. Recently, Wenger and Gray *et al* observed <sup>3</sup>MLCT emission of earth abundant low-valent Cr(0),<sup>13</sup> Mo(0)<sup>14</sup> and W(0)<sup>15</sup> complexes with arylisocyanide ligands.<sup>16</sup> Some of these complexes have been explored as photoredox catalysts in Diels-Alder reactions,<sup>7</sup> alkylations and oxidative cyclisations,<sup>17</sup> trifluoromethylation of alkenes,<sup>9</sup> and polymerization.<sup>2</sup> Much less explored as a strategy is the harnessing of LMCT states using electron-poor metals with electron-rich ligands.<sup>18</sup> Recently a Zr(IV) photocatalyst<sup>17a</sup> was reported for dehalogenation, reduction of olefins and reductive coupling. While this report is important, the value of the excited state oxidation potential is very small owing to the low energy of the excited state and thus its reduction power is weak.

Herein, we report the first examples of photoactive Co(III) complexes that were found to be deep blue luminescent at r.t. The two novel homoleptic Co(III) complexes, **1** and **2** incorporate six-membered chelate ligands **L1** (dgy) and **L2** (dgpz), respectively, that contain the strongly  $\sigma$ -donating hpp moiety (hpp = 1,3,4,6,7,8-hexahydropyrimido[1,2-a]pyrimidine) (**Scheme 1**).<sup>19</sup> **1** and **2** were found to be amongst the strongest photo-oxidants to date and this rare property was exploited in photoredox catalysis for regioselective mono(trifluoromethylation) of conjugated arenes as a proof of principle. The photocatalytic mechanism was found to proceed *via* a reductive quenching pathway that is distinct from the other earth-abundant photocatalysts reported to date.<sup>2</sup>

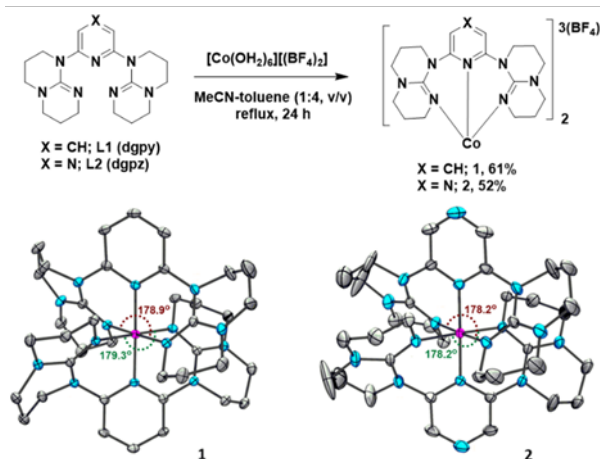
Ligands **L1** and **L2** were synthesized following literature procedures.<sup>19b-d</sup> The reactions of **L1** and **L2** with [Co(OH<sub>2</sub>)<sub>6</sub>][(BF<sub>4</sub>)<sub>2</sub>] in 2.2:1 stoichiometry provided **1**, [Co(**L1**)<sub>2</sub>][(BF<sub>4</sub>)<sub>3</sub>] and **2**, [Co(**L2**)<sub>2</sub>][(BF<sub>4</sub>)<sub>3</sub>] in good yields (**Scheme 1**). Due to the strong electron donating nature of **L1** and **L2**, **1** and **2** were isolated directly as oxidized Co(III) salts. To compare the redox and photophysical properties of **1** and **2**, a model complex, [Co(Ph-tpy)<sub>2</sub>][(PF<sub>6</sub>)<sub>3</sub>], **3** (Ph-tpy = 4'-phenyl-2,2':6',2''-terpyridine) was also synthesized (**Scheme S1**, ES1).

[a] Dr. A. K. Pal, Prof. G. S. Hanan  
Département de Chimie  
Université de Montréal  
Montréal, Québec, H3T 1J4, Canada  
E-mail: [garry.hanan@umontreal.ca](mailto:garry.hanan@umontreal.ca)

[b] Dr. A. K. Pal, Mr. C. Li, Dr. E. Zysman-Colman  
Organic Semiconductor Center, EaStCHEM School of Chemistry  
University of St Andrews  
St Andrews, Fife KY16 9ST, United Kingdom  
E-mail: [eli.zysman-colman@st-andrews.ac.uk](mailto:eli.zysman-colman@st-andrews.ac.uk)

Supporting information for this article can be found under:  
<https://doi.org/10.1002/anie.2018xxxxx>.

## COMMUNICATION



**Scheme 1.** Syntheses of **1** and **2**, with their ORTEP views (CCDC no. 1011784, 1011785). H atoms, anions, solvent molecules for **1** and **2** and a disordered part of the hpp moiety of **2** are omitted for clarity. Only one molecule in the asymmetric unit of **1** is shown. Ellipsoids correspond to 20% and 50% probability levels for **1** and **2**, respectively.

The low-spin nature of the Co(III) in **1** and **2** was confirmed by the diamagnetic nature of their  $^1\text{H}$  NMR spectra (Figures S1-S4 in ESI). The appearance of multiple peaks over 0-4 ppm region in  $^1\text{H}$  NMR spectra of **1** and **2** suggests that upon coordination the exchange between the equatorial and the axial protons in the saturated backbone of **L1** is slow compared to the NMR time scale.<sup>19</sup>

The electrochemical behavior of **1**, **2** and **3** have been examined by cyclic voltammetry (Figure S10-12 in ESI) and differential pulse voltammetry. The first oxidation and first reduction processes are mono-electronic. **1** and **2** show irreversible ligand-based oxidations at 1.75 and 1.98 V vs. SCE, respectively, assigned by DFT calculations (Figure 1 and Tables S3-S5 in ESI). The cathodic shift of  $E_{\text{ox}}$  of **1** vs. **2** is a function of the increased electron richness of **L1** compared to **L2**.

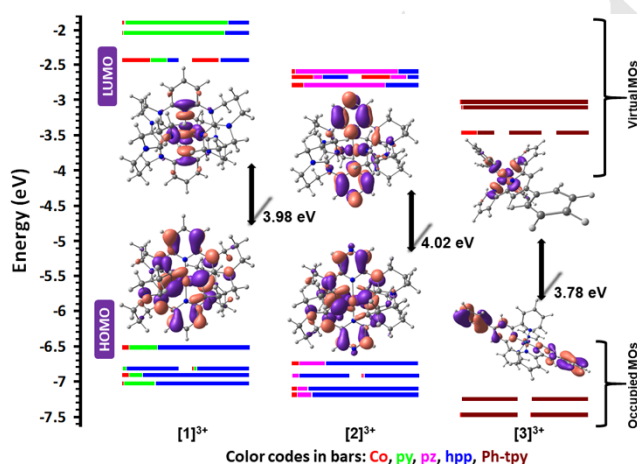


**Figure 1.** Calculated Kohn-Sham energy level diagram and electron density distribution images of the HOMO, LUMO of  $[1]^{3+}$ ,  $[2]^{3+}$  and  $[3]^{3+}$  using DFT calculations.

The higher energy calculated for the HOMO of **1** ( $E_{\text{HOMO}} = -6.49$  eV) compared to that of **2** ( $E_{\text{HOMO}} = -6.75$  eV) corroborates this trend. **1** and **2** exhibit quasi-reversible reduction waves at -0.58 V and -0.39 V, respectively. Based on the DFT calculations, the first reduction wave in **1** ( $E_{\text{LUMO}} = -2.51$  eV) is assigned to the Co(III)/Co(II) redox couple while for **2** ( $E_{\text{LUMO}} = -2.73$  eV) it is assigned to the reduction of the admixture of the pyrazine moiety and Co(III). The electron-poor nature of the pyrazine stabilizes the ligand-based reduction compared to the metal-based reduction in **1**.

The UV-vis absorption spectra of **1**, **2** and **3** in MeCN solutions display ligand-centered (LC)  $\pi \rightarrow \pi^*$  transitions around 220-330 nm (Figures S13-15 and Tables S6-S8 in ESI). Ligands **L1** and **L2** show lowest energy absorption bands at 311 and 340 nm, respectively.<sup>19b,d</sup> The low energy bands of **1**, **2** and **3** are assigned as a mixture of charge transfer transitions (see ESI for full assignments). The predicted oscillator strength values associated with the lowest energy singlet ligand-to-metal charge transfer ( $^1\text{LMCT}$ ) absorption transitions of **1** and **2** were found to be 0.0001 and 0.014, respectively (Tables S7 and S8, ESI).

**1** and **2** show unprecedented emission for Co(III) complexes at r.t. in degassed MeCN with emission maxima at

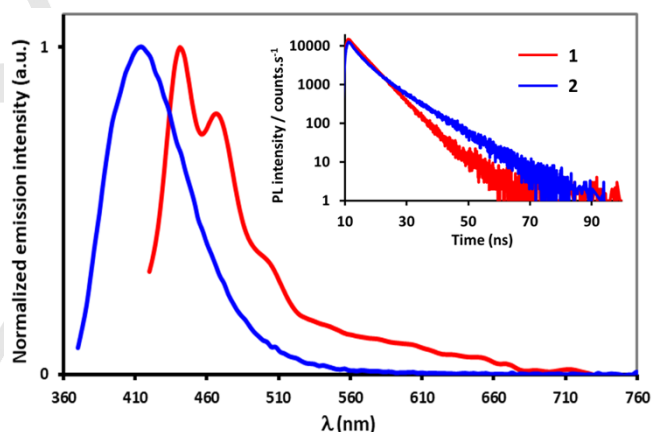


**Figure 2.** Photoluminescence spectra of **1** and **2** in dry, degassed MeCN ( $\lambda_{\text{exc}} = 360$  nm) at r.t. Inset shows the excited state decay profiles of **1** and **2** ( $\lambda_{\text{exc}} = 378$  nm) in dry, degassed MeCN at r.t.

440 and 412 nm, respectively (Figure 2 and Table S11 in ESI). Relevant photophysical data in MeCN, in butyronitrile matrix at 77 K and for 10 wt% polymethylmethacrylate film are provided in Tables S11 and S12 (ESI). Ligands **L1** and **L2** were reported to be UV-emissive at 360 and 382 nm, respectively, in deaerated MeCN.<sup>19b,d</sup> While **1** displays monoexponential emission decay in MeCN with a lifetime ( $\tau_{\text{PL}}$ ) of 5.07 ns at r.t., the emission decay of **2** is biexponential with  $\tau_{\text{PL}}$  of 3.21 (39%) and 8.69 (61%) ns (Figure 2). The photoluminescence quantum yields ( $\Phi_{\text{PL}}$ ) were found to be 0.70% and 0.40% for **1** and **2**, respectively in degassed MeCN at r.t. while in aerated MeCN the  $\Phi_{\text{PL}}$  values of **1** and **2** are reduced to 0.40% and 0.12%, respectively. The similar  $\Phi_{\text{PL}}$  values of **1** and **2** are in line with the similar  $k_r$  and  $k_{nr}$  values calculated for **1** and **2** (Table S11, ESI). The spin density

## COMMUNICATION

distributions of **1** and **2** are located mostly on the Co(III) ion, with some contribution from the central heterocycle of the hpp ligands (**Figure S17**, ESI). Based on the O<sub>2</sub>-sensitive nature of the emission, its origin in **1** is attributed to a triplet <sup>3</sup>LMCT state. The bi-exponential decay profile in **2** suggests that the emission of **2** arises from a different excited state than that of **1**. In comparison to an isoelectronic Fe<sup>II</sup>-NHC (NHC = N-heterocyclic carbene) complex ( $E_{T1} \sim 1240$  nm,  $\tau_{PL} = 528$  ps) the  $\tau_{PL}$  values of **1** and **2** (**Table S12**, ESI) are found to be  $\sim 950$  times higher, presumably in part due to the very low energy of the triplet state in the iron complex.<sup>20</sup> By contrast, **3** exhibits no emission. Thus, the combination of 6-membered chelates and electron-rich ligands is key to turn on the emission in Co(III) complexes by separating the <sup>3</sup>LMCT and/or <sup>3</sup>LC states from the non-radiative <sup>3</sup>MC state.

**1** and **2** exhibit blue-shifted emission at 437 nm and 395 nm, respectively, in butyronitrile matrices at 77 K compared to those in MeCN solutions at r.t., substantiating the CT nature of the emission at r.t. (**Table S11**, ESI). The emission maxima of the 10 wt% doped films in PMMA of **1** and **2** are 410 nm and 398 nm, respectively, with average  $\tau_{PL}$  values of  $\sim 5$  ns (**Table S12**, ESI). Similar to the trends observed in MeCN, the thin film  $\Phi_{PL}$  under degassed condition for **2** at 0.8% is similar to that found for **1** at 1.1%. (**Table S12**, ESI). The emission maxima and  $\tau_{PL}$  values of **1** and **2** in doped films at 77 K were found to be similar to those at r.t. (**Table S12**, ESI). The excited state oxidation and reduction potentials,  $E_{Ox}^*$  and  $E_{Red}^*$ , respectively, were calculated as  $E_{Ox}^* = -1.26$  V and  $-1.15$  V and  $E_{Red}^* = 2.26$  and  $2.75$  V vs. SCE, for **1** and **2**, respectively (**Table S13**, ESI).<sup>21</sup> **1** and **2** possess significantly higher  $E_{Red}^*$  values compared to those of benchmark photocatalysts such as [Ru(bpy)<sub>3</sub>]<sup>2+</sup> ( $E_{Red}^* = 0.77$  V),<sup>2</sup> [Ir(dF(CF<sub>3</sub>)ppy)<sub>2</sub>(dtbubpy)]<sup>+</sup> (where dF(CF<sub>3</sub>)ppy = 2-(2,4-difluorophenyl)-5-(trifluoromethyl)pyridinato-C<sup>2</sup>,N'), ( $E_{Red}^* = 0.89$  V),<sup>22</sup> [Cr(Ph<sub>2</sub>phen)<sub>3</sub>]<sup>3+</sup> (where Ph<sub>2</sub>phen = 4,7-diphenyl-1,10-phenanthroline) ( $E_{Red}^* = 1.40$  V),<sup>2</sup> triphenylpyrylium ( $E_{Red}^* = 2.30$  V)<sup>23</sup> and mesityl diaminoacridinium ( $E_{Red}^* = 1.25$  V)<sup>24</sup> thus making **1** and **2** amongst the strongest photo-oxidants identified to date (**Table S13**, ESI).

Considering the favorable excited state redox properties, we were interested in the unexplored field of photochemical regioselective mono(trifluoromethylation) of PAHs as a first proof of concept. In the context of organic transformations, trifluoromethylation of alkenes and arenes is particularly topical for its wide use of trifluoromethylated compounds in medicinal,<sup>25</sup> agro-industrial<sup>26</sup> and material chemistry<sup>27</sup> (**Figure 4**). The pioneering work of trifluoromethylation of PAHs is based on the reaction of these arenes with trifluoroiodomethane (CF<sub>3</sub>I) under harsh reaction conditions (T = 360 °C, flame sealed ampoule) to afford multiple regioisomers and poor chemoselectivity as a result of poly(trifluoromethylation) (**Figure 4**).<sup>28</sup> Recently, Harris *et al* reported photoinduced radical C-H (hetero)aryl mono(trifluoromethylation) of substituted-benzene/furan/thiophene as an application in small molecule transformation.<sup>29</sup> To the best of our knowledge, photocatalytic mono(trifluoromethylation) on PAHs has not yet been reported due to the lack of a suitable photocatalyst.

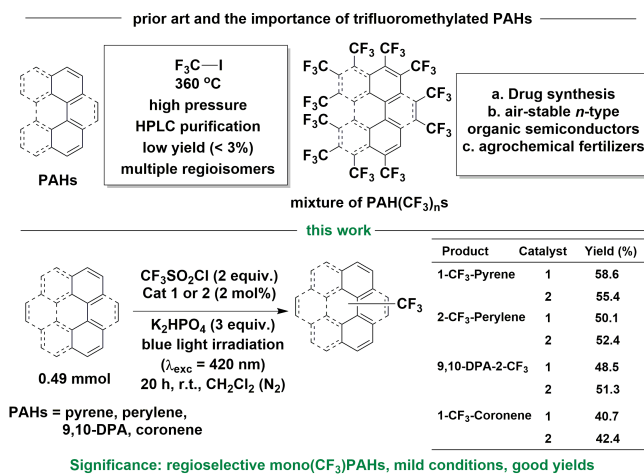


**Figure 4.** Prior art of trifluoromethylation,<sup>28</sup> importance of trifluoromethylated-PAHs and significance of this work.

The experimental conditions of our trifluoromethylation reaction are mentioned in **Figure 4** (see also **Figure S18** in ESI). TfCl was used for trifluoromethylation instead of CF<sub>3</sub>I to avoid any competitive aryl iodination because of CF<sub>3</sub>-I homolysis.<sup>30</sup> Under these conditions pyrene, perylene, 9,10-DPA and coronene were each active to chemoselective trifluoromethylation (**Figure 4**, see **Figures S19-S21** for NMRs in ESI). Arenes such as benzene, naphthalene and phenanthrene were unreactive, suggesting that the substrate also acts as a photosensitizer. The presence of **1** or **2**, the requirement for light irradiation and the choice of base as K<sub>2</sub>HPO<sub>4</sub> were all necessary for reaction progression. The use of K<sub>2</sub>CO<sub>3</sub> as the base or its removal resulted undesired products as monitored by the comparison of the NMR spectra of the crude reaction mixtures (**Figure S22**, ESI). Replacement of **1** or **2** with a commonly used Ir(III) photocatalyst [Ir(dF(CF<sub>3</sub>)ppy)<sub>2</sub>(bpy)]<sup>+</sup>[PF<sub>6</sub>]<sup>-</sup> ( $E_{Red}^* = 1.32$  V)<sup>31</sup> resulted in significantly poorer chemoselectivity, giving rise to multiple trifluoromethylated regioisomeric products, regardless the arene substrates used, all of which were found to be practically inseparable (**Figure S23**, ESI).

A plausible reaction mechanism, using pyrene as the substrate and **1** as the photoredox catalyst, is depicted in **Figure 5**. Notably, the PAHs are themselves photoactive and can participate as photosensitizers.<sup>32,33</sup> At first, excitation of pyrene occurs to its triplet state (**1**) by means of energy transfer from the excited state of **1**.<sup>34</sup> Oxidative quenching via single-electron transfer (SET) of TfCl to form TfCl<sup>•+</sup> followed by fragmentation results in the generation of <sup>•</sup>CF<sub>3</sub>, **3**,<sup>30</sup> with concomitant formation of the pyrenyl radical cation, **2**.<sup>33</sup> The formation of the stable radical <sup>•</sup>CF<sub>3</sub>, **3** is entropically driven by the release of SO<sub>2</sub> and chloride.<sup>30</sup> This SET process is supported by the more negative excited state oxidation potential, calculated for pyrene ( $E_{Ox}^{*T} = -1.26$  V vs. SCE) compared to the reduction potential of the TfCl ( $E_{Ox} = -0.18$  V vs. SCE)<sup>30</sup> and Stern-Volmer quenching of the emission of pyrene as a function of gradual addition of TfCl (**Table S14** and **Figure S24** in ESI). The electron-deficient <sup>•</sup>CF<sub>3</sub> radical is then well-suited to add to the most electron-rich position of pyrene in a regioselective fashion. The resultant CF<sub>3</sub>-pyrenyl radical, **4**



## COMMUNICATION

then undergoes a second SET event with the excited photocatalyst, **5** (here denoted as  $^*[\text{ML}_2]^{3+}$ , where M = Co and L = **L1** or **L2**) to generate the reduced photocatalyst  $[\text{ML}_2]^{2+}$ , **6** and  $\text{CF}_3$ -pyrenyl cation, **7**. The formation of **6** is supported by *in situ* reaction monitoring by UV-vis spectroscopy with the evolution of the band at 291 nm, which is a signature of  $[\text{ML}_2]^{2+}$ , itself independently obtained *via* chemical reduction of  $[\text{ML}_2]^{3+}$  in the presence of excess hydrazine monohydrate (Figures S25 and S26, ESI). The two photocatalytic cycles are closed via a third SET wherein **2** is reduced to pyrene and **6** is oxidized to  $[\text{ML}_2]^{3+}$ . Finally, facile deprotonation of **7** with  $\text{K}_2\text{HPO}_4$

as the base affords the desired  $\text{CF}_3$ -pyrene. Reaction kinetics for mono(trifluoromethylation) of pyrene using complex **1** was found to be slower, but results in a cleaner conversion to the product when compared to the similar kinetics using  $[\text{Ir}(\text{dF}(\text{CF}_3)\text{ppy})_2(\text{bpy})][\text{PF}_6]$  as the photoredox catalyst (Figures S27-28, ESI). The two-photon excitation mechanism is supported by a quadratic dependency of the product yield on irradiation density as assessed by quantitative  $^{19}\text{F}$  NMR spectroscopy (Figures S29 and S30, ESI).

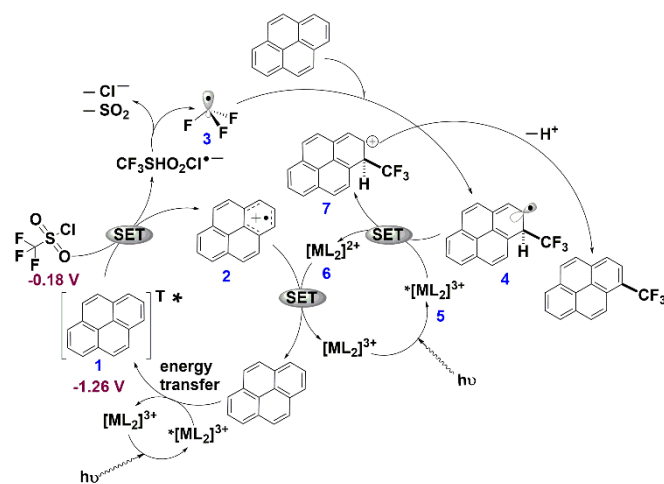


**Figure 5.** Proposed mechanism of trifluoromethylation of PAHs. Values in maroon report the  $E_{\text{Red}}$  and  $E_{\text{Ox}}^*$  of  $\text{CF}_3\text{SO}_2\text{Cl}$  and pyrene, respectively.

In conclusion, the need for abundant, cheap, low toxicity and environmentally friendly photocatalysts make **1** and **2** attractive alternatives to the more commonly used photocatalysts based on Ru(II) and Ir(III). Notably, Co(III)-based photocatalysts can become viable only when very electron-rich 6-membered chelate ligands such as **L1** and **L2** are employed. **1** and **2** were found to be deep blue emissive. These are very rare examples of LMCT emissive complexes with high excited state energy. **1** and **2** were used as photoredox catalysts for the selective trifluoromethylation of four different  $\pi$ -conjugated arenes to afford mono(trifluoromethylated) arenes in good yield. These earth-abundant Co(III) complexes represent some of the most powerful photo-oxidants reported to date.

## Acknowledgements

A.K.P and G.S.H thank Natural Sciences and Engineering Research Council of Canada and Dr. Mihaela Cibian for recording the UV-vis absorption spectrum of **3**. A.K.P thanks the Leverhulme Trust Early Career Fellowship (ECF-2017-326) and the University of St Andrews. We thank the Prof. & Mrs Purdie Bequests Scholarship and AstraZeneca support for C.L. EZ-C thanks the Engineering and Physical Sciences Research Council (EP/M02105X/1) and the University of St Andrews. We thank the EPSRC UK National Mass Spectrometry Facility at Swansea University for analytical services.

## Conflict of interest

The authors declare no conflict of interest.

**Keywords:** Emissive Co(III) complexes • Electrochemistry • DFT calculations • Photophysics • Photoredox catalysis

1. a) T. P. Yoon, M. A. Ischay, J. Du, *Nat. Chem.* **2010**, *2*, 527-532; b) J. M. R. Narayanan, C. R. J. Stephenson, *Chem. Soc. Rev.* **2011**, *40*, 102-113; c) C. K. Prier, D. A. Rankic, D. W. C. MacMillan, *Chem. Rev.* **2013**, *113*, 5322-5363.
2. C. B. Larsen, O. S. Wenger, *Chem. Eur. J.* **2018**, *24*, 2039-2058 and references cited therein.
3. D. M. Arias-Rotondo, J. K. McCusker, *Chem. Soc. Rev.* **2016**, *45*, 5803-5820.
4. A. K. Pal, G. S. Hanan, *Chem. Soc. Rev.* **2014**, *43*, 6184-6197.
5. a) B. Schulze, D. Escudero, C. Friebe, R. Siebert, H. Gçrls, S. Sinn, M. Thomas, S. Mai, J. Popp, B. Dietzek, L. González, U. S. Schubert, *Chem. Eur. J.* **2012**, *18*, 4010-4025; b) D. G. Brown, N. Sanguantrakun, B. Schulze, U. S. Schubert, C. P. Berlinguette, *J. Am. Chem. Soc.* **2012**, *134*, 12354-12357.
6. a) L. Hammarström, O. Johansson, *Coord. Chem. Rev.* **2010**, *254*, 2546-2559 and references cited therein; b) M. Abrahamsson, M. Jäger, T. Österman, L. Eriksson, P. Persson, H.-C. Becker, O. Johansson, L. Hammarström, *J. Am. Chem. Soc.* **2006**, *128*, 12616-12617; c) S. Otto, M. Grabolle, C. Förster, C. Kreitner, U. Resch-Genger, K. Heinze, *Angew. Chem. Int. Ed.* **2015**, *54*, 11572-11576.
7. S. Otto, A. M. Nauth, E. Emilov, N. Scholz, A. Friedrich, U. Resch-Genger, S. Lochbrunner, T. Opatz, K. Heinze, *ChemPhotoChem* **2017**, *1*, 344-349.
8. P. Chåbera, Y. Liu, O. Prakash, E. Thyraug, A. E. Nahhas, A. Honarfar, S. Essén, L. A. Fredin, T. C. B. Harlang, K. S. Kjær, K. Handrup, F. Ericson, H. Tatsuno, K. Morgan, J. Schnadt, L. Häggström, T. Ericsson, A. Sobkowiak, S. Lidin, P. Huang, S. Styring, J. Uhlig, J. Bendix, R. Lomoth, V. Sundström, P. Persson, K. Wärnmark, *Nature*, **2017**, *543*, 695-699.
9. a) A. C. Hernandez-Perez, S. K. Collins, *Acc. Chem. Res.* **2016**, *49*, 1557; b) O. Reiser, *Acc. Chem. Res.* **2016**, *49*, 1990-1996.
10. S. Malzkuhn, O. S. Wenger, *Coord. Chem. Rev.* **2018**, *359*, 52-56.
11. S. Shanmugam, J. Xu, C. Boyer, *J. Am. Chem. Soc.* **2015**, *137*, 9174-9185.
12. L. X. Chen, G. B. Shaw, I. Novozhilova, T. Liu, G. Jennings, K. Attenkofer, G. J. Meyer, P. Coppens, *J. Am. Chem. Soc.* **2003**, *125*, 7022-7034.
13. a) L. A. Büldt, X. Guo, R. Vogel, A. Prescimone, O. S. Wenger, *J. Am. Chem. Soc.* **2017**, *139*, 985; b) L. A. Büldt, O. S. Wenger, *Chem. Sci.* **2017**, *8*, 7359-7367.
14. L. A. Büldt, X. Guo, A. Prescimone, O. S. Wenger, *Angew. Chem. Int. Ed.* **2016**, *55*, 11247-11250.
15. W. Sattler, L. M. Henling, J. R. Winkler, H. B. Gray, *J. Am. Chem. Soc.*, **2015**, *137*, 1198-1205.

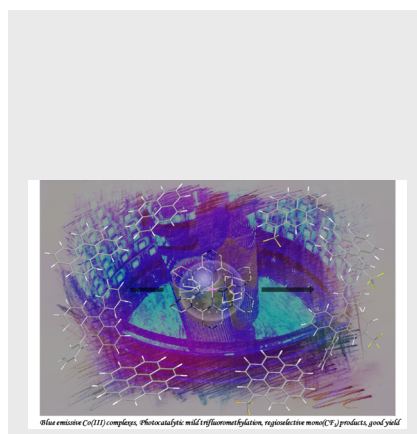
## COMMUNICATION

16. L. A. Büldt, O. S. Wenger, *Angew. Chem. Int. Ed.* **2017**, *56*, 5676-5682.
17. a) A. Gualandi, M. Marchini, L. Mengozzi, M. Natali, M. Lucarini, P. Ceroni, P. G. Cozzi, *ACS Catal.* **2015**, *5*, 5927-5931; b) S. Parisien-Collette, A. C. Hernandez-Perez, S. K. Collins, *Org. Lett.* **2016**, *18*, 4994-4997.
18. a) Y. Zhang, J. L. Petersen, C. Milsmann, *J. Am. Chem. Soc.* **2016**, *138*, 13115-13118; b) K. T. Yeung, W. P. To, C. Sun, G. Cheng, C. Ma, G. S. M. Tong, C. Yang, C. M. Che, *Angew. Chem. Int. Ed.*, **2017**, *56*, 133-137; c) S. Gazi, W. K. H. Ng, R. Ganguly, A. M. P. Moeljadi, H. Hirao, H. S. Soo, *Chem. Sci.* **2015**, *6*, 7130-7142.
19. a) A. K. Pal, S. Nag, J. M. Ferreira, V. Brochery, G. L. Ganga, A. Santoro, S. Serroni, S. Campagna, G. S. Hanan, *Inorg. Chem.* **2014**, *53*, 1679-1689; b) A. K. Pal, N. Zaccheroni, S. Campagna, G. S. Hanan, *Chem. Commun.* **2014**, *50*, 6846-6849; c) A. K. Pal, S. Serroni, N. Zaccheroni, S. Campagna, G. S. Hanan, *Chem. Sci.* **2014**, *5*, 4800-4811; d) A. K. Pal, G. S. Hanan, *Dalton Trans.* **2014**, *43*, 11811-11814; e) A. K. Pal, P. D. Dauphin, G. S. Hanan, *Chem. Commun.* **2014**, *50*, 3303-3305; f) A. K. Pal, G. S. Hanan, *Dalton Trans.* **2014**, *43*, 6567-6577.
20. P. Chábera, K. S. Kjaer, O. Prakash, A. Honarfar, Y. Liu, L. A. Fredin, T. C. B. Harlang, S. Lidin, J. Uhlig, V. Sundström, R. Lomoth, P. Persson, K. Wärnmark, *J. Phys. Chem. Lett.* **2018**, *9*, 459-463.
21. D. M. Arias-Rotondo, J. K. McCusker, *Chem. Soc. Rev.* **2016**, *45*, 5803-5820.
22. M. S. Lowry, J. I. Goldsmith, J. D. Slinker, R. Rohl, R. A. Jr. Pascal, G. G. Malliaras, S. Bernhard, *Chem. Mater.* **2005**, *17*, 5712-5719.
23. D. A. Nicewicz, T. M. Nguyen, *ACS Catal.* **2014**, *4*, 355-360.
24. C. Fischer, C. Sparr, *Angew. Chem. Int. Ed.* **2018**, *57*, 2436-2440.
25. a) K. Muller, C. Faeh, F. Diederich, *Science* **2007**, *317*, 1881-1886.
26. P. Jeschke, *ChemBioChem* **2004**, *5*, 570-589.
27. Z. Yuan, Y. Xiao, Z. Li, X. Qian, *Org. Lett.* **2009**, *11*, 2808-2811.
28. I. V. Kuvychko, K. P. Castro, S. H. M. Deng, X.-B. Wang, S. H. Strauss, O. V. Boltalina, *Angew. Chem. Int. Ed.* **2013**, *52*, 4871-4874.
29. C. F. Harris, C. S. Kuehner, J. Bacsa, J. D. Soper, *Angew. Chem. Int. Ed.* **2018**, *57*, 1311-1315.
30. D. A. Nagib, D. W. C. MacMillan, *Nature* **2011**, *480*, 224-228.
31. D. Hanss, J. C. Freys, G. Bernardinelli, O. S. Wenger, *Eur. J. Inorg. Chem.* **2009**, 4850-4859.
32. S. Okamoto, R. Ariki, H. Tsujioka, A. Sudo, *J. Org. Chem.*, **2017**, *82*, 9731-9736.
33. N. Noto, T. Koike, M. Akita, *Chem. Sci.* **2017**, *8*, 6375-6379.
34. M. Brasholz, *Angew. Chem. Int. Ed.* **2017**, *56*, 10280-10281.

## COMMUNICATION

## COMMUNICATION

**'Cobalt Blue'**: First examples of room temperature blue emissive Co(III) complexes are presented. The low negative first reduction potential and the high excited state energies made them strong photooxidant. They are successfully adapted in the photoredox trifluoromethylation of polycyclic aromatic hydrocarbons (PAHs).



Amlan K. Pal, Chenfei Li, Eli Zysman-Colman\* and Garry S. Hanan\*

Page No. – Page No.

**Blue Emissive Cobalt(III) Complexes and Their Use in the Photocatalytic Trifluoromethylation of Polycyclic Aromatic Hydrocarbons**

Accepted Manuscript